LCLS-II Technical Note

Beam shaping with a passive linearizer at the LCLS-II for high-current operation

LCLS-II TN-18-02

6/25/2018

Y. Ding[1], K. Bane[1], P. Emma[1], Z. Guo[1], Z. Huang[1], J. Qiang[2], W. Qin[3] and G. Stupakov[1]

1. SLAC
2. LBNL
3. Peking University

Abstract:

In this note we discuss an idea of using a passive, corrugated structure for the purpose of fine tuning the final LCLS-II current profile. In simulations a corrugated structure is added early in the LCLS-II beamline—specifically, right after the first chicane bunch compressor, where higher-order time-energy correlation in the chirped beam can be flexibly controlled. By optimizing the corrugated structure parameters, the linac RF phases, and the compressor parameters, we find that the final current profile can be made smoother, with a higher core peak, than can be achieved without the structure. We report here the initial, promising simulation results; we intend to develop this idea further in future work.

1 Introduction

In LCLS-II x-ray FEL pulses will be generated having high *average* brightness at a megahertz-level repetition rate, opening up remarkable, new capabilities for various scientific research fields. However, improving the FEL pulse *peak* brightness at high repetition rate also engenders much interest from fields such as single-molecule imaging and nonlinear x-ray science. The electron beam quality is the most important factor affecting the radiation pulse peak brightness; typically what is required is an electron beam with low emittance and high current. While the (slice) emittance is determined at the gun, high peak current can be achieved by longitudinal compression of the electron bunch.

For the LCLS-II driven by superconducting linacs, the electron bunch, coming from a very-high-frequency (VHF) gun, has a lower peak current and a lower energy than what is achieved at the present (normal conducting) S-band RF gun of LCLS-I. To achieve a final peak current in LCLS-II at the kA-level, a stronger compression is required. However, the achievable peak current is limited by strong nonlinearities in single particle and collective effects in the linacs and bunch compressors. For example, according to the present LCLS-II design, at 100 pC bunch charge, the peak current is about 800 A [1]. The future high energy upgrade of LCLS-II, the LCLS-II-HE, will operate at shorter wavelengths using an 8-GeV CW electron beam. High peak current is even more critical for the LCLS-II-HE FEL performance. This motivates us to develop methods for high-current operation at the LCLS-II.

At the LCLS-I, which is based on a normal-conducting, copper linac, the maximum beam repetition rate is 120 Hz. There, a beam shaping scheme—one that utilizes a transverse collimator at the first bunch compressor—has been used to truncate the inevitable current horns that appear at the head and tail of the bunch [2]. With a more uniform final current profile, stronger compression becomes possible, leading to the achievement of higher FEL peak power [3]. Unfortunately, such a shaping scheme is not applicable to the LCLS-II due to the high radiation loss and other safety concerns connected with collimating the high repetition-rate beam.

We here propose the idea of adding a dechirper-like corrugated structure in the low energy region of the LCLS-II linac, where it can function as a passive, phase space linearizer and helps to customize the beam

energy chirp before it enters the second bunch compressor. After optimizing the parameters of the system, we found that it is possible to enhance the compression factor in the final bunch compressor and thus to achieve a higher final peak current. Note also that, with this method, the current profile can be shaped to avoid large spikes at the head and tail of the distribution. In this technical note we will present initial results on the passive linearizer studies for LCLS-II.

2 Corrugated structure for passive linearization

Beam-induced wakefields in a linac are unavoidable and need to be included in the system design studies of a linac-based x-ray FEL. For example, the longitudinal wakefield in the copper linac of the LCLS reduces the beam chirp that we need to induce for compression, and also causes a third-order time-energy correlation that leads to a double-horn structure in the final beam current distribution. On the other hand, wakefields can also be used for beam phase space manipulation or chirp control. One popular device for this purpose is a corrugated structure, also called a "dechirper"—since it was proposed to cancel residual energy chirp in a beam [4]. For example, a dechirper has been used for chirp control at the PAL test facility [5] and at the LCLS [6]. At the Shanghai SDUV-FEL, the dechirper was used as a linearizer at the end of the linac, for bandwidth control [7]. Recently, PSI colleagues proposed putting a corrugated structure before the first bunch compressor in an FEL, in order to induce chirp modulation for generating two-color FEL pulses [8]. Besides using the longitudinal wakefield for chirp control, the transverse wakefield of the corrugated structure has also been used for fresh-slice lasing control with various applications at the LCLS [9]. At the Fermi-FEL, a study has reported using the wakefield of a high-impedance accelerating structure for phase space linearization, without the need of additional devices [10].

LCLS-II is a superconducting, high repetition-rate, linac-based FEL (the layout is shown in Figure 1). It includes an injector; L1, a 1.3-GHz SRF linac section; L1H, a 3.9-GHz, SRF harmonic section; a first bunch compressor, BC1; L2, a 1.3-GHz SRF linac section; a second bunch compressor, BC2; a long bypass line; and two undulator beamlines. We propose to add a corrugated structure right after BC1 as a passive linearizer.

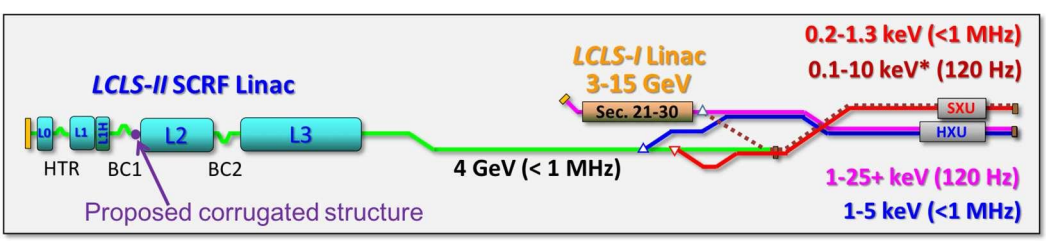

Figure 1: Layout of the LCLS-II. The proposed corrugated structure is positioned right after BC1.

The LCLS-II rms bunch length, after BC1, is about 0.2 mm in the case of bunch charge of 100 pC. There are recent developments in the theory and formulation of wakefields in corrugated structures [11]. For the relatively long bunches considered here, the wakefields obtained by perturbation calculation should

be applied [12]. We use a solution in terms of simplified fitting parameters, presented by Stupakov [13], for our wakefield calculations.

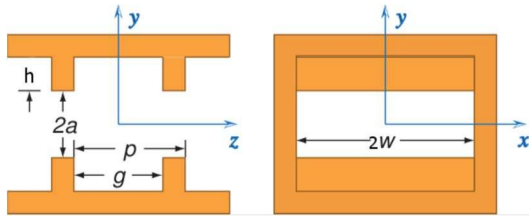

Figure 2: Geometry of the corrugated structure, in longitudinal cut (left) and transverse cut (right).

The geometry of the corrugated structure is shown in Figure 2. We consider the case structure width $\boldsymbol{w} \gg \boldsymbol{a}$. For a typical case, we also assume the corrugation dimensions are much smaller than the half gap $\boldsymbol{a}$: $\boldsymbol{p}, \boldsymbol{h} \ll \boldsymbol{a}$, and the depth of corrugation is comparable or large compared to the period, $\boldsymbol{h} \gtrsim \boldsymbol{p}$. Under these assumptions, the longitudinal wakefield can be approximated as [13]:

$w_{\parallel}(s) = \frac{Z_0 c}{4\pi}\frac{2}{a^2}F(s/\lambda_0)$, with $\lambda_0 = \frac{2\pi c}{\omega_{min}}$, and $F(x) = b_1 e^{-b_2 x}\cos(b_3 x + b_4 x^2)$.

Here $\boldsymbol{\omega_{min}} = \frac{\boldsymbol{c}}{\sqrt{\boldsymbol{ha}(\boldsymbol{\mu} - {}^{-1})}}$ is the minimum frequency for the resonant mode, $\boldsymbol{\mu} = \boldsymbol{g}/\boldsymbol{p}$. To find $\boldsymbol{\epsilon}$ one needs to solve an electrostatic problem [14]. In typical cases the effect of $\boldsymbol{\epsilon}$ is small; we ignore it here. The four fitting parameters are: b_1 = 1.2638, b_2 = 0.3713, b_3 = 7.1126, b_4 = -0.2432.

The transverse wakefields with fitting parameters are also derived in [13]; however, in this technical note, we focus on the longitudinal wakefield, and optimize the beam final current and phase space. We checked the transverse wakefield effects using Elegant simulations, which will be discussed later.

3 Simulation studies

The LCLS-II beam is generated in a VHF gun (the APEX-type gun) with beam energy ~750 keV; it is then passed through a buncher for compression; then it is accelerated to ~100 MeV in the first cryomodule. The low energy beam in the injector is studied and optimized using the Impact-T code [15]. For our downstream tracking and optimization, we use as input the particle distribution at 100 MeV obtained by Impact-T simulations.

Three different codes have been used in our study, tracking from the injector exit (before the laser heater) to the entrance of the undulator: LiTrack [16], Elegant [17], and Impact-Z [18]. Matlab-based LiTrack is a longitudinal phase space tracking code that includes acceleration, compression and the effect of wakefields from an RF structure or a chamber's resistive-wall wake. Coherent synchrotron radiation (CSR), with a steady-state model, is available but we ignore it here, for simplicity. LiTrack tracking is fast and can be easily combined with multi-objective optimization. We adopted the Non-dominated Sorting Genetic Algorithm (NSGA) in the optimization process. The variables include the L1/L3 linac phases, the 3rd harmonic RF structure (L1H) amplitude and phase, the compression factors of BC1 and BC2, and the dechirper parameters. The energy at the two compressors can also be varied if necessary.

The optimization target is a high core current, a uniform current profile, and minimum beam chirp. One optimized configuration (using LiTrack) for a 100-pC bunch charge is summarized in Table 1.

Table 1: An optimized machine setup with bunch charge of 100 pC.

Parameters	**value**	**unit**
Laser Heater (rms)	6	keV
L1 phase	-25.68	deg
L1H amplitude	40.5	MV
L1H phase	-169.1	deg
L2 phase	-26.7	deg
BC1 energy	220	MeV
BC1 R_{56}	-53.3	mm
BC2 energy	1.615	GeV
BC2 R_{56}	-59	mm
Corrugated structure 2*a*	1	mm
Corrugated structure *p*	100	um
Corrugated structure *g*	50	um
Corrugated structure *h*	66	um
Corrugated structure length	0.25	m

We show in Figure 3 simulation results from LiTrack: (a) the initial, longitudinal beam properties at 100 MeV (we used a 2016 version injector beam from Impact-T), (b) the beam after the corrugated structure (which is located right after BC1), and (c) the final beam at 4 GeV just before the undulator. We see that the final peak beam current is over 1 kA, and the current profile does not have strong spikes at the head or tail.

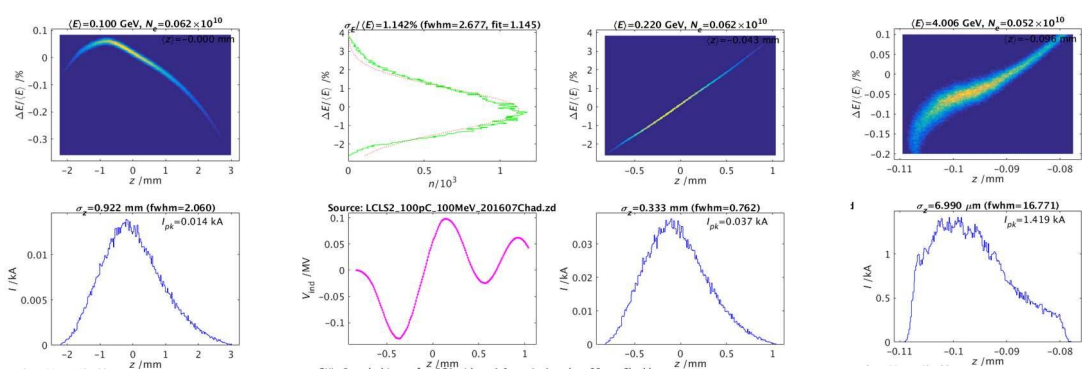

(a) Initial beam out of injector

(b) Right after the corrugated structure after BC1

(c) Final beam at the undulator entrance

Figure 3: The LiTrack simulation results for 100-pC charge with the optimized parameters given in Table-1. Bunch head is to the left.

Based on the optimized solution using LiTrack (Table 1), we set up Elegant and Impact-Z simulations,

including all the collective effects available in the codes. For example, the 1-D CSR model is activated in both codes, as is the 1-D longitudinal space charge (LSC) force in Elegant and the 3-D space charge force in Impact-Z. In Elegant, we used 10^7 macro particles, while in Impact-Z, the number of macro particles equals the real number of electrons, ~6.25×10^8. We show the final tracking results in Figure 4, with those of Elegant on the left, and those of Impact-Z on the right. We can see that the two codes give very similar results for phase space and current profile. Note that in Elegant, we didn't tweak any parameters of Table 1. In Impact-Z, small tweaks (less than 2%) of the BC2 R_{56} value have been made, to achieve a similar current profile as in Elegant. The initial (normalized) emittance at the injector output (with 100% particles) is about 0.32 μm for both x and y. For the final projected emittance, Elegant gives $\varepsilon_x = 0.56\,\mu\text{m}$, $\varepsilon_y = 0.32\mu\text{m}$, while Impact-Z gives $\varepsilon_x = 0.48\,\mu\text{m}$, $\varepsilon_y = 0.41\mu\text{m}$. In Elegant the final vertical emittance is preserved, while in Impact-Z, the vertical emittance also increases, probably due to the transverse space charge force. We also see that CSR causes some ripple in the core part of the bunch. The final current, according to Figure 4, is slightly lower than the LiTrack result of Figure 3; most likely this is due to a smaller induced chirp, caused by the combination of the CSR and LSC effects.

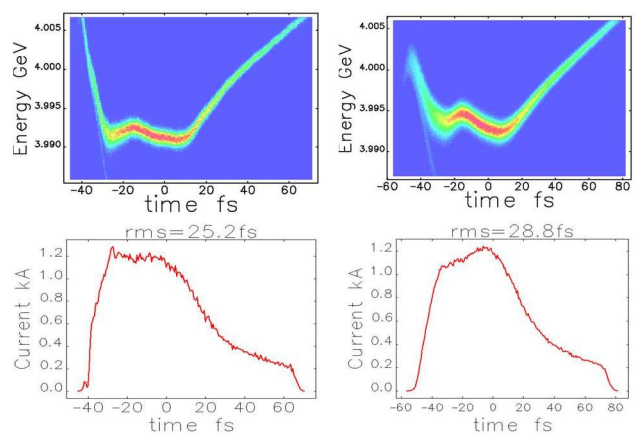

Figure 4: Beam at the entrance of the undulator according to Elegant (left) and Impact-Z (right) simulations. The machine setup is based on Table 1. The bunch head is to the left.

In Elegant we also checked the transverse wake effect. We chose a location in the beamline with a small beta function (beta functions ~10 m), where the transverse wakefield effect from the structure was negligible. As a practical detail, note that the best configuration would use two corrugated structures with orthogonal layout (one is horizontal and one is vertical), so that the time-dependent focusing effect from the quadrupole wakefield can be made to cancel out.

As a comparison to earlier work, we show some baseline LCLS-II simulation results from the Impact-Z code (without the corrugated structure). Using the same injector beam (as shown in Figure 3(a)), the optimized final beam from Impact-Z simulations, with the baseline LCLS-II parameters, is shown in Figure 5, as reported in 2016 FAC review by Mitchell and Qiang [19]. To see the shaping effect, the result in Figure 4 (right) should be compared with that in Figure 5, where they both used the same injector beam and

are tracked with Impact-Z. We can see the improvement in Figure 5 with a corrugated structure. Further Impact optimizations with the LCLS-II baseline setup have been carried out by Qiang et al. in 2017. With the 2017 setup, the injector is further optimized and the time-energy correlation in the 100-MeV beam at the injector output is slightly different from the 2016 one. When we use this new injector beam for passive linearizer optimization, we see the final results are similar but the energy wiggle of CSR in phase space is stronger with a longer tail in the current profile, and the optimized machine setup has been changed as well. The sensitivity and requirements for the initial beam when using a passive linearizer should be studied further.

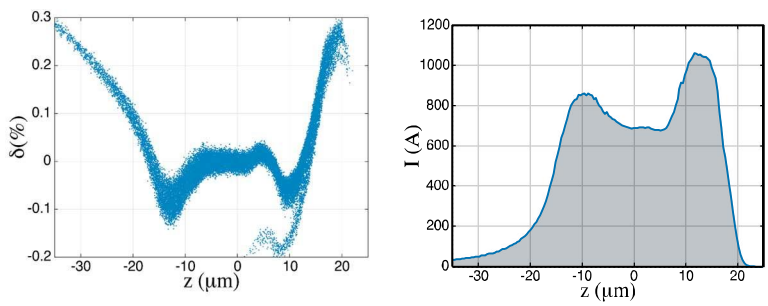

Figure 5: Optimized simulation results from Impact-Z for the baseline LCLS-II configuration without the corrugated structure. This used the same 2016 initial injector beam as used in this tech-note study shown in Fig. 3(a). Left: the final longitudinal phase space; Right: the current profile. Note here the bunch head is to the right. (Results are from Mitchell and Qiang, LBNL).

4 Discussion

Based on initial investigations with a corrugated structure for passive linearization at the LCLS-II, we obtain encouraging results of improved peak current and a smoother beam shape. We see that, when using a 0.25-m long, corrugated structure after BC1, the final core current can be increased from 800 A to 1200 A, and with an improved current profile. Impact-Z simulations, with the number of the macro particles equal to the real number of electrons, confirmed these results.

Further studies are still needed, including the tolerance on the corrugated structure parameters and the sensitivity to variations in the initial beam properties out of the injector. Since the RF structure wakefield of the superconducting linacs is small, the initial beam time-energy correlation out of the injector plays a very important role in this passive linearization scheme. The optimal location of the corrugated structure can also be further investigated. Note also that the gap between the two plates of the dechirper structure is adjustable, a property that can be used to change the strength and the fundamental mode period of the wakefield. To make it more flexible, however, one might consider tapering the structure depth h in the transverse direction (horizontal in Figure 2). Then, by adjusting the horizontal position of the beam in the structure, we can control the parameter depth h. Combined with the adjustable gap $2a$, we can have two knobs, gap and depth, for controlling the wavelength independent of the amplitude of the induced wake.

Higher currents than what we show in Figure 4 seem to be possible, but the CSR effect in BC2 and in the downstream bending magnets will then become stronger, causing more energy ripple in longitudinal phase

space. Methods for suppressing the CSR effect should also be considered. In this initial test of concept we chose a fixed value for bunch charge (100 pC); in future work other values of bunch charge will be considered to confirm the feasibility of passive linearization over a range of bunch population.

References:

[1] LCLS-II Final Design Report.

[2] Y. Ding et al., "Beam shaping to improve the FEL performance at the LCLS", Physical Review Accelerator and Beams, 19, 100703 (2016).

[3] M. Guetg et al., "Generation of high power high intensity short x-ray FEL pulses", Physical Review Letters 120, 014801 (2018).

[4] K.L.F. Bane, G. Stupakov, "Corrugated Pipe as a Beam Dechirper", Nucl.Instrum.Meth. A690 (2012) 106-110.

[5] P. Emma et al., "Experimental Demonstration of Energy-Chirp Control in Relativistic Electron Bunches Using a Corrugated Pipe", Phys. Rev. Lett. 112, 034801 (2014).

[6] T. Maxwell et al., "Demonstration of Energy-Chirp Control in Relativistic Electron. Bunches at LCLS Using a Corrugated Structure", NAPAC 2016.

[7] H.X. Deng et al., "Experimental Demonstration of Longitudinal Beam Phase-Space Linearizer in a Free-Electron Laser Facility by Corrugated Structures", PRL 113, 254802 (2014).

[8] S. Bettoni, E. Prat, and S. Reiche, "Two-color beam generation based on wakefield excitation", PRAB 19, 050702 (2016).

[9] A. Lutman et al., "Fresh-slice multicolor x-ray Free-electron lasers", Nature Photonics, 10, 745 (2016).

[10] G. Penco et al., "Passive Linearization of the Magnetic Bunch Compression Using Self-Induced Fields", Phys. Rev. Lett. 119, 184802 (2017)

[11] see, for example, Karl Bane, Gennady Stupakov, and Igor Zagorodnov, "Analytical formulas for short bunch wakes in a flat dechirper", Phys. Rev. Accel. Beams 19, 084401 (2016), and references there.

[12] K. Band and G. Stupakov, "Impedance of a rectangular beam tube with small corrugations", PRST-AB 6, 024401 (2003).

[13] G. Stupakov, "Rectangular dechirper theory", NGLS-SLAC meeting report (not published?), 2012.

[14] G. Stupakov, K. L. F. Bane, "Surface Impedance Formalism for a Metallic Beam Pipe with Small Corrugations", SLAC-PUB-15213.

[15] Ji Qiang, Steve Lidia, Robert D. Ryne, and Cecile Limborg-Deprey, "Three-dimensional quasistatic model for high brightness beam dynamics simulation," Phys. Rev. ST Accel. Beams 9, 044204 (2006).

[16] K. Bane and P. Emma, in Proceedings of the 21st Particle Accelerator Conference, PAC2005, Knoxville, TN, 2005. (IEEE, Piscataway, NJ, 2005), p. 4266.

[17] M. Borland, “elegant: A Flexible SDDS-Compliant Code for Accelerator Simulation,” Advanced. Photon Source LS-287, September 2000.

[18] J. Qiang et al., “High resolution simulation of beam dynamics in electron linacs for x-ray free electron lasers”, Phys. Rev. ST Accel. Beams 12, 100702 (2009).

[19] C. Mitchell and J. Qiang, internal report 2016.